Monazite end members and solid solutions: synthesis, unit-cell characteristics, and utilization as microprobe standards*

THE synthesis of monazite was first reported by Radominsky (1875). Since then various methods have been used to synthesize various end members of the monazite solid solution series, mainly $CePO_4$ and $LaPO_4$ (e.g. Anthony, 1957, 1965). As part of an experimental study dealing with the solubility of monazite in granitic melts (Montel, 1986, 1987, and in prep.), the synthesis of some of the end members, as well as solid solutions, was achieved.

Experimental procedure. A *RE* hydroxide gel was precipitated by ammonia (5 cm³ NH_4OH) from an aqueous solution of $RECl_3$ (3 g $RECl_3$ in 100 ml H_2O), and then dried for 24 hours at room temperature. For solid solutions, a complex gel was made by precipitating all *RE* hydroxides from the same solution. The synthesis was made by reaction, without water, of a molar excess of H_3PO_4 with the gel. It was performed both in

* C.R.P.G. contribution no. 746.

hydrothermal bombs at low *T* and *P*, and in externally heated cold-seal vessels under various conditions (Table 1).

Results. Run conditions and results are summarized in Table 1. Monazite was obtained in all runs, despite the very different experimental conditions. End members, a simple La-Ce solid solution, and a complex solid solution were obtained. Low-pressure, low-temperature runs yielded small crystals mostly with no visible crystal faces. Better results were obtained in gold crucibles (5 cm long) at 600 °C and 3000 bars, using cold-seal vessels with a temperature gradient (Table 1). Under these conditions, euhedral, transparent, and coloured, crystals of monazite (Table 1 and Fig. 1) were produced in one week for Pr-, Nd-, Sm-, and Gd-monazite. The complex gel yielded a complex monazite, also well crystallized. Electron microprobe investigations showed that this monazite is homogeneous. Its composition is reported in Table

Table 1. Experimental conditions and results

Name	Apparatus	T(°C)	P(bar)	Time(days)	Size	Colour	Observations
Ce-1	Cold-seal	200	300	2	3µm	colourless	Crystal faces visible with MEB
Ce-2	Autoclave	220	?	2	2µm	"	Rare large crystals without crystal face
Ce-3	Cold-seal	300	500	2	2µm	"	No face visible with microscope
Ce-4	Cold-seal	200	200	7	2µm	"	Some well crystallized specimens
Ce-5	Autoclave*	220	?	2	2µm	"	No face visible with microscope
La-1	Cold-seal	200	200	2	2µm	"	" " " " "
La-Ce+	"	200	200	2	2µm	"	" " " " "
La-2	"	600(G)	3000	7	2mm	"	Small crystals with euhedral shape
Ce-6	"	600(G)	3000	7	0.3mm	"	" " " " "
Pr-1	"	600(G)	3000	7	1mm	green	All crystals with euhedral shape
Nd-1	"	600(G)	3000	7	4mm	purple	" " " " "
Sm-1	"	600(G)	3000	7	3mm	yellow	" " " " "
Gd-1	"	600(G)	3000	7	2mm	colourless	" " " " "
Complex	"	600(G)	3000	7	2mm	pink	" " " " "

* with excess water added; + initially 50% mole Ce, 50% mole La; (G) means that a temperature gradient is established in the crucible.
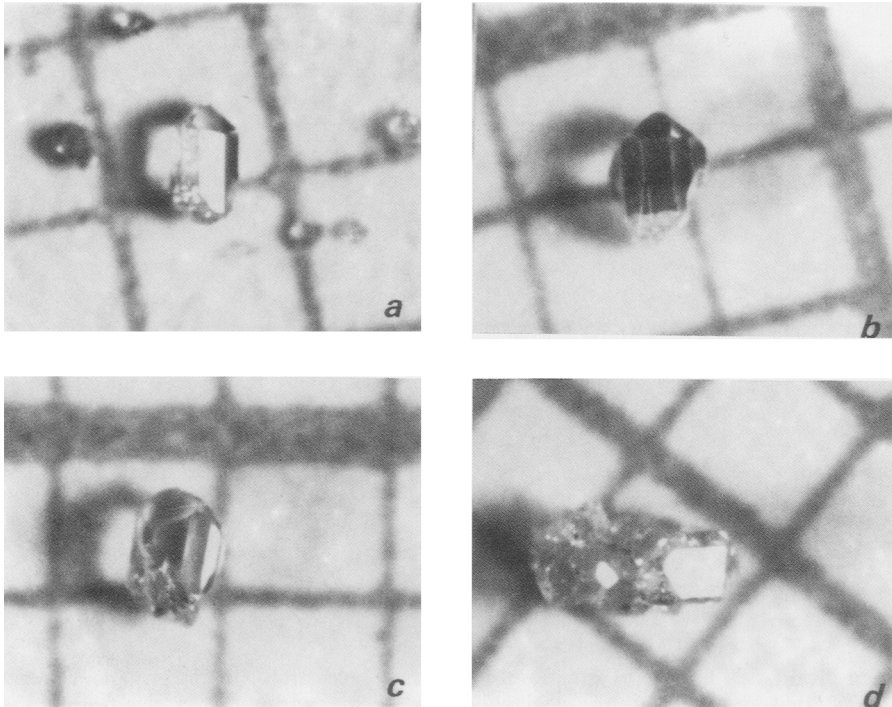
FIG. 1. Examples of synthetic crystals of monazite. Squares in the background are 1 mm wide; (*a*) run Sm-1; (*b*) run Nd-1; (*c*) and (*d*) complex monazite.

2. The *RE* were analysed by ICP, except Pr which was analysed by microprobe (as was P). Ce-monazite crystals were smaller, but equally well crystallized, whereas La ones were larger with less well developed faces.

X-ray diffractograms (monochromatized Cu-$K\alpha$ radiation) were obtained and well resolved peaks indexed by comparison with ASTM charts. Accurate determinations were performed on the 3000 bar, 600 °C set only. Each end member has an X-ray pattern identical to the corresponding mono-clinic *RE*-phosphate of the ASTM charts. All have very similar patterns, but peaks are shifted, indicating a diminution of the unit-cell size, from $LaPO_4$ to $GdPO_4$. The *d* (120) for example, changes from 3.12 Å for $LaPO_4$, to 3.03 Å for $GdPO_4$.

Cell parameters were calculated by least-squares fit of the peaks positions, 16 to 29 peaks being used. Results are summarized in Table 3: they agree with the ASTM references. The cell parameters *a*, *b*, and *c* decrease progressively, and almost linearly with decreasing ionic radius of the rare-earth, whereas the *β* angle increases slightly. The cell parameters of the complex monazite are similar to that of natural monazite (Deer *et al.*, 1962). No structural changes occur from $LaPO_4$ to $GdPO_4$, except the diminution of the size of the unit-cell. This suggests that the solid solutions between phosphates of *RE* of similar ionic radius (e.g. Ce

Table 2. Composition of the complex monazite

	wt%	atoms
La_2O_3	15.17	0.221
Ce_2O_3	31.90	0.461
Pr_2O_3	3.07	0.044
Nd_2O_3	16.34	0.230
Sm_2O_3	2.15	0.029
Gd_2O_3	1.53	0.020
P_2O_5	29.87	0.997
Total	100.03	

Structural formula based on four oxygens.

TABLE 3. Cell-parameters of synthetic monazites

sample	a	b	c	beta	V
La-1	6.8944(83)	7.0712(51)	6.4933(67)	103.521(95)	307.78(38)
La-2	6.8429(31)	7.0809(25)	6.5002(35)	103.289(54)	306.53(17)
Ce-1	6.7875(29)	7.0184(29)	6.4633(37)	103.507(43)	299.38(17)
Ce-3	6.8083(61)	7.0230(34)	6.4617(56)	103.505(70)	300.42(28)
Ce-5	6.8042(24)	7.0373(35)	6.4679(38)	103.532(36)	301.11(17)
Ce-6	6.8011(26)	7.0250(22)	6.4726(23)	103.493(34)	300.72(13)
Pr-1	6.7716(42)	6.9912(37)	6.4372(26)	103.603(44)	296.20(17)
Nd-1	6.7492(33)	6.9635(21)	6.4079(40)	103.713(52)	292.57(19)
Sm-1	6.6945(40)	6.8931(27)	6.3569(41)	103.897(59)	284.75(21)
Gd-1	6.6413(35)	6.8471(34)	6.3230(51)	104.035(57)	278.95(21)
La-Ce	6.8024(43)	7.0475(55)	6.4768(80)	103.340(80)	302.12(35)
Complex	6.7851(29)	7.0184(33)	6.4704(38)	103.392(53)	299.75(20)

$\underline{a}$, $\underline{b}$, $\underline{c}$, are in Å; beta is in degrees; $\underline{V}$ is in Å^3

and La) are ideal. As a first approximation, one may consider that monazite is an ideal solid solution for its major components Ce, La, and Nd. Departure from ideality is possible for more divergent ionic radii (e.g. La–Gd).

Uses of synthetic crystals. In experimental studies synthetic monazites may be used as analogues of natural minerals. The absence of zoning, the known composition, and the limited number of elements in the crystal are useful features. Complex monazites can be used as standard for the chemical analysis of natural monazites. For example, the analysis of monazites by electron microprobe is made difficult by two problems. First, their Ce, La, and Nd content are much higher than that of commonly used standards like Drake and Weill's (1972) glasses. The second and much more important problem is that no strong X-ray peaks exists for Nd, which does not overlap the peak of another *RE*. Correct analysis of Nd is difficult, so that its content in monazite is often overestimated and must be empirically corrected. These problems could be circumvented by use of a natural monazite of known composition as a standard, but unfortunately natural monazites are usually zoned. Alternatively, one can use a synthetic monazite, of composition similar to that of a natural monazite. Because the overlapping of the Nd peaks has a similar amplitude for both standard and sample, and because natural monazites have a broadly constant composition, satisfactory analyses can be obtained without correction. This method has

been successfully used at Nancy University for two years, and improves significantly the quality of the analyses of natural monazite.

References

Anthony, J. W. (1957) Hydrothermal synthesis of monazite. *Am. Mineral.* **42**, 904.
——(1965) Crystal morphology of thorium-bearing synthetic monazite. Ibid. **50**, 1421–31.
Deer, W. A., Howie, R. A., and Zussman, J. (1962) *Rock-forming minerals* vol. 5, 363 pp., Longmans, London.
Drake, M. J., and Weill, D. F. (1972) New rare-earth elements standard for electron microprobe analysis. *Chem. Geol.* **10**, 179–81.
Montel, J. M. (1986) Experimental determination of the solubility of Ce-monazite in SiO_2–Al_2O_3–K_2O–Na_2O melts at 800 °C, 2 kb, under H_2O-saturated conditions. *Geology*, **14**, 659–62.
——(1987) *Comportement des terres rares dans les magmas granitiques: modélisation et approche expéri-*

mentale du rôle de la monazite. Thèse de l'Institut
National Polytechnique de Lorraine, 117 pp.
Radominsky, M. F. (1875) Reproduction artificielle de
la monazite et de la xénotime. C. R. Acad. Sci. Paris,
80, 304-7.

Centre de Recherches Petrographiques et Géochimiques,   J. M. MONTEL*
B.P. 20, 54501, Vandoeuvre Les Nancy Cedex, France   F. LHOTE

Université de Nancy I, 54500, Vandoeuvre les Nancy, France   J. M. CLAUDE

* Present Address: CNRS, U.A.10, 5 rue Kessler, 63000 Clermont Ferrand, France.

Dahllite and whitlockite from Amatuku islet, Tuvalu

PHOSPHATIC limestones and a related soil were described from collections made by the first Royal Society coral-reef-boring expedition to Funafuti in 1896 (Cooksey, 1896; David and Sweet, 1904; Judd, 1904; Sollas, 1904; cf. Cullis, 1904). Although there is some geographic uncertainty about the source of some of Judd's samples, the specimens came from three localities on Funafuti, the largest being on Amatuku.

Occurrence. Amatuku is a small (550 × 180 m) arcuate islet in the north of Funafuti atoll (lat: 8° 31′ S; long: 179° 12′ E). Apart from the phosphatic rocks, the entire islet consists of bioclastic Quaternary calcareous sediments and limestones. The main occurrence of phosphatic rock is 80 m from the westernmost tip of the islet. From here, Sollas (1904, p. 24-5) described phosphatic limestone forming a low cliff reaching almost two metres above sea level on the lagoon coast. This cliff is now eroded but phosphatic limestones are exposed beneath low tide and extend to the top of the islet's terrace with small residual phosbergs (cf. Stoddart and Scoffin, 1983) jutting out within a gravel-strewn beach. Above the intertidal zone a jumble of broken phosphatic blocks extend across the 20 m width of the island in a 25 m wide band. On the ocean coast the phosphatic horizon is less than half a metre thick and confined to the supratidal terrace with a thin, indurated phosphatic layer coating the storm wave platform. In addition to this main locality, small knobs of brown, phosphatic limestone outcrop throughout central and western Amatuku.

Petrography. The 3-4° WNW dip which Sollas recorded for the lagoon coast beds is that of phosphatic biocalcarenties and biocalcirudites forming the phosbergs. Texturally the rocks are grainstones with sorting being moderate to good within any one layer. In the rudites, rounded clasts commonly vary up to 12.5 cm but the main range is between 20 and 60 mm. Arenites are well rounded, medium to coarse sands in which granules consisting of entire tests of calcarinid and soritinid foraminifera are frequent (Fig. 1a). Fines are rare to absent.

In a typical, highly porous, fine biocalcirudite, the granule- and pebble-sized clasts are cemented by a thin (0.02-0.05 mm), microlaminated, botyroidal phosphatic crust which evenly coats grains and intraskeletal cavities (Figs 1a, b). At high magnifications the crust often appears as globular clusters coated in a reticulated web of ill-defined crystallites. In thin section the crust shows from five to fifteen layers of extremely fine-grained, translucent collophane, tinted pale yellow to brown, weakly anisotropic and with r.i. greater than balsam (Fig. 1c). Individual laminae forming the layers are about 0.005 mm thick and rarely show microfibrous texture. Bioclasts show no replacement by phosphate nor is there evidence of pre-existing carbonate cement(s) nor of replacement of such cement(s). The textural relationships of the Amatuku rocks conform to those of Stoddart and Scoffin's (1983, p. 386) Group I: 'Phosphates cementing unaltered carbonate grains.'

The colour of the cement ranges from tan to dark brown, the darkest colours occurring amongst sub-aerial samples. One rock from the intertidal zone was bright pink when first collected. Within twenty-four hours the dry specimen had